Available online at www.CivileJournal.org

Civil Engineering Journal

Vol. 5, No. 10, October, 2019

Non-Smooth Behavior of Reinforced Concrete Beam Using Extended Finite Element Method

Eman Abbas [a], Alaa H. Al-Zuhairi [a*]

[a] *Department of Civil Engineering, Collage of Engineering, University of Baghdad, AL-Jadriha, Baghdad, Iraq.*

Received 13 May 2019; Accepted 17 September 2019

Abstract

Flexure members such as reinforced concrete (RC) simply supported beams subjected to two-point loading were analyzed numerically. The Extended Finite Element Method (XFEM) was employed for the treatment the non-smooth h behaviour such as discontinuities and singularities. This method is a powerful technique used for the analysis of the fracture process and crack propagation in concrete. Concrete is a heterogeneous material that consists of coarse aggregate, cement mortar and air voids distributed in the cement paste. Numerical modeling of concrete comprises a two-scale model, using mesoscale and macroscale numerical models. The effectiveness and validity of the Meso-Scale Approach (MSA) in modeling of the reinforced concrete beams with minimum reinforcement was studied. ABAQUS program was utilized for Finite Element (FE) modeling and analysis of the beams. On the other hand, mesoscale modeling of concrete constituents was executed with the aid of ABAQUS PYTHON language and programing using excel sheets. The concrete beams under flexure were experimentally investigated as well as by the numerical analysis. The comparison between experimental and numerical results showed that the mesoscale model gives a better indication for representing the concrete models in the numerical approach and a more appropriate result when compared with the experimental results.

Keywords: Extended Finite Element Method; Mesoscale Modeling; Reinforced Concrete Beams; Non-Smooth Behaviour.

1. Introduction

Concrete is the most widely used construction material because of its versatility, durability, sustainability and economy. Concrete is a mixture of aggregates and sand held together by a binder of cementitious paste. The paste is typically made up of Portland cement and water and may also contain supplementary cementing materials (SCMs), such as fly ash or slag cement, and chemical admixtures. To represent the mechanical behavior of this material precisely, it must be treated as a multiphase material, and its behavior should be like material like concrete as a result from the behavior of these components taken together. Many scales in modeling are used to represent the heterogynous material like concrete such as macro, meso and micro scale modelling. In the traditional numerical modeling, concrete was modelled using the macroscale, whereas, microscale modeling was used in very limited cases. The mesoscale is a scale that falls between the macro-and micro-scales [1]. In this paper, two reinforced concrete beams with dimension (350×200×2200) mm were subjected to two-point loads and analyzed numerically using the XFEM. The results of this analysis were compared with the experimental results of the same reinforced concrete beam with approximately the same composition.

In general, meso-scale modeling can be classified into two types: (1) The continuum models, (2) The lattice models.

* Corresponding author: alaalwn@coeng.uobaghdad.edu.iq

http://dx.doi.org/10.28991/cej-2019-03091408

© 2019 by the authors. Licensee C.E.J, Tehran, Iran. This article is an open access article distributed under the terms and conditions of the Creative Commons Attribution (CC-BY) license (http://creativecommons.org/licenses/by/4.0/).

In the first model, concrete is modeled as a continuum composite material consisting of aggregate, mortar, and the interface zone between the two materials [2], while in the second model, the concrete is assumed as a discrete system consist of a lattice element [3]. The lattice modeling method needs a huge numerical effort to obtain the concrete meso-structure acceptable for the analysis. In this paper, the continuum mesoscale model was used to model concrete, where concrete is partitioned into two phases, aggregate and mortar. Mortar contains air voids that result from the pouring process of concrete. The interface between the aggregate and cement mortar in the numerical model was modeled as fully bounded and tied that make the two materials assumed fully consistent.

On the other hand, the mesoscale modeling has two approaches:

1. The image-based modeling, and;
2. The parameterization modeling.

The first approach is built up on a set of two-dimensional pictures that are assembled together to have a three-dimensional model, then the numerical model is conducted based on this three-dimensional model. This approach is an accurate method for modeling the concrete with a shortcoming that is expensive and is a time consuming method [4-6].

The second approach can be classified into two methods direct and indirect. The direct method modeled the aggregate particles with various physical properties such as size, shape and orientation, gradation and distribution of the aggregate particles. The aggregate particles are assumed to be floating in the cement mortar. This method is more appropriate for the mesoscale modeling process. The indirect method modeled the concrete randomly using a suitable finite element mesh, or using the lattice modeling for aggregate and mortar [7-9].

In this paper, the direct method for the parameterization approach was used for the modeling of concrete to study the non-smooth behavior of RC beams. This study aims to investigate the significance of the MSA in RC modeling using XFEM. In addition, the validity of this method to treat the heterogeneity nature of concrete during analysis of beams will be confirmed.

2. The Extended Finite Element Method (XFEM)

The conventional Finite Element Method (FEM) is ideally appropriate to the approximation of smooth solutions that depend on the approximation properties of polynomials but lacks the accuracy and convergence rate when the exact solution of differential equations or its gradients have singularities or discontinuities. These solutions required high computational cost and had numerical difficulties.

The Extended Finite Element Method (XFEM) is a numerical method, based on the FEM that is especially designed for treating discontinuities and singularities. Discontinuities are generally divided into strong and weak discontinuities [10-11]. Strong discontinuities result from displacement jumps such as cracks and holes, while weak discontinuities result from jumping in the strains such as bi-material problems. On the other hand, the fractured domain causes a singularity in the stress field at the crack tip region. XFEM is a powerful and an accurate approach used to model these problems [12] (see Figure 1).

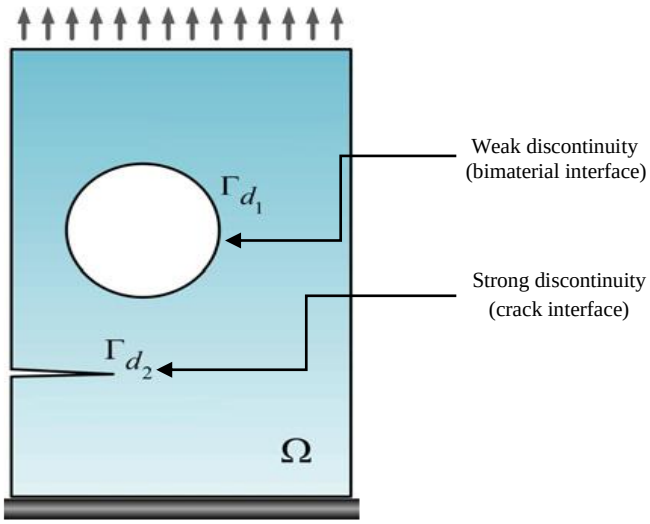

Figure 1. Weak and strong discontinuities [12]

In the FEM, the approximation displacement field takes the form:

$$u(x) = \sum_{i=1}^{N} N_i(x) \times \bar{u}_i \quad (1)$$

Where:

$u(x)$: Displacement;

$N_i(x)$: The standard shape functions;

$\bar{u}_i$: The FE degree of freedom (standard D.O.F) or (standard nodal displacement);

N: The set of all nodal points.

The XFEM is based on the enrichment of the approximation field by adding the enrichment terms to the standard or regular interpolation as shown in Equation 1.

$$u(x) = \sum_{i=1}^{N} N_i(x) \times \bar{u}_i + enrichment\ terms \quad (2)$$

$$u(x) = \underbrace{\sum_{i=1}^{N} N_i(x) \times \bar{u}_i}_{\text{Regular interpolation}} + \underbrace{\sum_{k=1}^{p} \bar{N}_i(x) \times \left(\sum_{j=1}^{M} \psi_j(x) \times \bar{a}_{ij}\right)}_{\text{Enrichment interpolation}} \quad (3)$$

Where:

$\bar{a}_i$: Enrichment DOF;

M: The number of enrichment nodes;

$\psi_j(x)$: The enrichment function;

p: The number of enrichment functions.

3. Enrichment Function

The level set function can be used as an enrichment function if the discontinuity results from differences in the types of material properties (weak discontinuity). The level set function is the signed distance function $\varphi(x)$

$$u_{\text{weak discontinuity}}(x) = \sum_{i=1}^{N} N_i(x) \times \bar{u}_i + \sum_{j=1}^{M} N_j(x) \times (|\varphi(x)| - |\varphi(x_j)|) \times \bar{a}_j \quad (4)$$

$$\varphi(\vec{x}) = \vec{N}\, d(\vec{x}) \quad (5)$$

$$\varphi(x) \begin{cases} > 0 \text{ if } \vec{x} \in \Omega A \\ = 0 \text{ if } \vec{x} \in \Gamma d \\ < 0 \text{ if } \vec{x} \in \Omega B \end{cases} \quad (6)$$

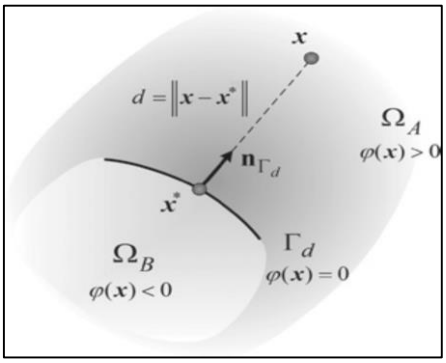

Figure 2. The signed distance function [12]

Where:

$\varphi(\vec{x})$: is the signed distance to the closest point on the interface (see Figure 2);

$\vec{N}$: is the local unit normal at $\vec{x}$ takes the value (+ or -) that referred to outside region and inside region. Then $\varphi(\vec{x})$ can be written as shown in Equation 7:

$$\varphi(x) = d(x)\, sign\left(n_{\Gamma d}(x - x_c)\right) = |x - x_c| sign\left(n_{\Gamma d}(x - x_c)\right) \quad (7)$$

$$sign\left(n_{\Gamma d}(x - x_c)\right) = \vec{N}$$

Where:

$n_{\Gamma d}$: is the normal vector to the interface at point x_c

For modeling of cracks (strong discontinuity) one of the two types of enrichment functions can be used Heaviside or Step function (jump function) and Asymptotic near-tip enrichment functions [12], and [13].

$$u_{crack}(x) = \sum_{i\in N} N_i(x) \times \bar{u}_i + \sum_{j\in N^{dis}} N_i(x) \sum_{j=1}^{M} N_j(x) \times \left(H(x) - H(x_j)\right) \times \bar{d}_j + \sum_{k\in N^{tip}} N_k(x) \times \sum_{a=1}^{4} (B_a(x) - B_a(x_k)) \times \bar{b}_{ak} \quad (8)$$

Where:

N^{dis}: The set of enriched nodes whose support is bisected by the crack;

N^{tip}: The set of nodes which contain the crack tip in the support of their shape functions enriched by the asymptotic functions;

$\bar{u}_i$: The unknown standard nodal DOF at I^{th} node;

$\bar{d}_j$: The unknown enriched nodal DOF associated with the Heaviside enrichment function at node J;

$\bar{b}_{ak}$: The additional enriched nodal DOF associated with the asymptotic functions at node K.

When a crack cut some elements it split the domain into two parts. This splitting of the domain causes a displacement jump. The Heaviside function $H(x)$ is used to model the crack discontinuity in the XFE formulation. There are two ways proposed to define the Heaviside function to represent the crack. The first way is named as Heaviside step function as shown in Equation 9, and the second way is generally referred to as the Heaviside sign function with the mathematical formulation as shown in Equation 10.

$$H(x) = \begin{cases} 0 \text{ if } \varphi(x) < 0 \\ 1 \text{ if } \varphi(x) > 0 \end{cases} \quad (9)$$

$$H(x) = \begin{cases} -1 \text{ if } \varphi(x) < 0 \\ 1 \text{ if } \varphi(x) > 0 \end{cases} \quad (10)$$

Where:

$\varphi(x)$: The signed distance function;

$$\varphi(x) = d(x)\,\vec{N} = |x - x_c|\,\vec{N} \quad (11)$$

x : The point under query;

x_c: The nearest point to the crack segment Γ_d;

$\vec{N}$: The unit normal vector at x_c.

4. Experimental Investigation

Two reinforced concrete beams were studied in this study. Rounded coarse aggregate with maximum size of 25 mm was used in both of these beams. The only difference between the beams is concentrated in their compressive strengths, that is, 17 and 26 MPa. Two-point loading system for a RC concrete beams with minimum reinforcement ratio (see Figure 3) was produced for the experimental study using the concrete mixes illustrated in Table 1. The dimensions, boundary conditions, and loading system are illustrated in Figure 4.

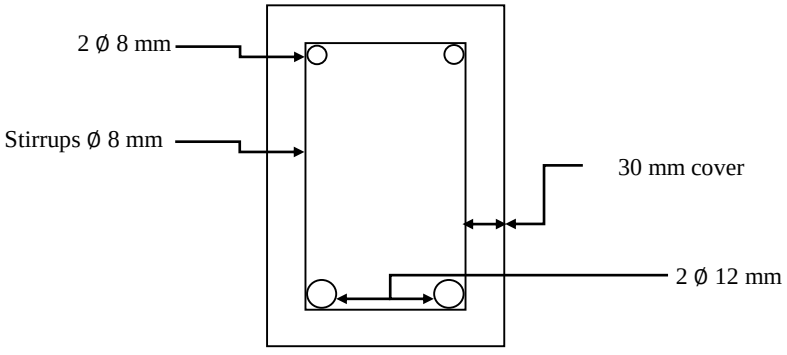

Figure 3. Section in the beam model

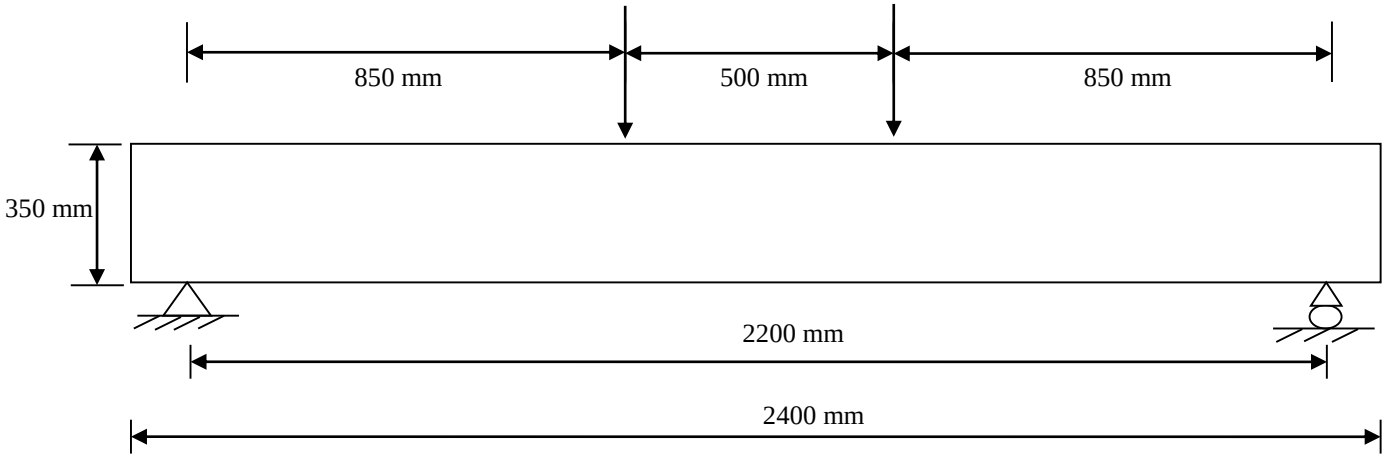

Figure 4. Reinforced concrete beam model

Table 1. Concrete mix proportions for the concrete beam specimens

	Beam Code No.	
	17-M 25-R	**34-M 25-R**
Cement kg/m^3	257	399
Coarse Aggregate kg/m^3	1249	1249
Fine Aggregate kg/m^3	610	490
Mixing Water kg/m^3	193	193
Air Voids Content %	1.5	1.5
Density of Coarse Aggregate	1720	1720

The coding of the RC beams used in this study is illustrated below:

Coding example: a-M b-c (see Table 2)

Where: (a) denotes the compressive strength of concrete; (b) denotes the maximum size of coarse aggregate; (c) denotes the type of the coarse aggregate used (crushed, or rounded).

Table 2. Beams code numbers

Maximum size of the coarse aggregate	Compressive Strength, MPa	Beam Code No.
25	17	17-M 25-R
	34	34-M 25-R

Five Electric strain gauges were fixed on each RC beam specimen, the first strain gauge was fixed in the middle of the front face at the tension zone. The second one was placed at the middle of the center line of the bottom face. These two strain gauges were used to measure the tensile strain at mid-span caused by applied bending moment (see Figure 5). The other three strain gauges were placed in the shear zone at the midpoint of the distance between the top and bottom faces. These strain gauges were fixed so that their ends met at one point (see Figure 6). The purpose of this arrangement is to create a strain rosette by which the shear strain can be measured. Two dial gauges of accuracy 0.002 mm were used for deflection measurement. The first one was placed at the mid-span of the bottom face of the specimens for the maximum deflection measurement. The second one was used to measure the lateral buckling (note: the beams were designed without lateral buckling but this dial gauge was placed for checking; see Figure 7). Then the beams are placed in the frame structure for load application (see Figure 8).

Figure 5. Strain gauge distribution

Figure 6. Strain gauges attachment rosette

Figure 7. Dial gauges placed for deflection measurement

Figure 8. Testing setup

5. Finite Element Modelling Using ABAQUS Software Program

ABAQUS program was used for the modeling and analysis of the RC beam specimens. The mesoscale finite element modeling for RC beams have round coarse aggregate with maximum size 25 as explained in Figure 9. Concrete is one kind of heterogeneous composite material consisting of coarse aggregates, cement mortar, mortar-aggregate interface, and pores at the meso-level [14, 15]. In this study, the concrete is represented as a two-phasic material (aggregate, and cement mortar). The interface between two consisting materials was assumed fully bonded interface. Perfect bonding between the concrete and steel bar will be assumed [16].

Air voids were assumed to be space voids in the concrete model without any material properties. Concrete is considered as a linear elastic material, i.e., the stress-strain curve of the concrete is approximately a linear function. The mesoscale materials properties were selected according to Bazant (2014) [19]. The damage evaluation was considered according to the input of the fracture energy (see Table 3). As it can be seen in Table 3, the crack is assumed to propagate through cement mortar only [9].

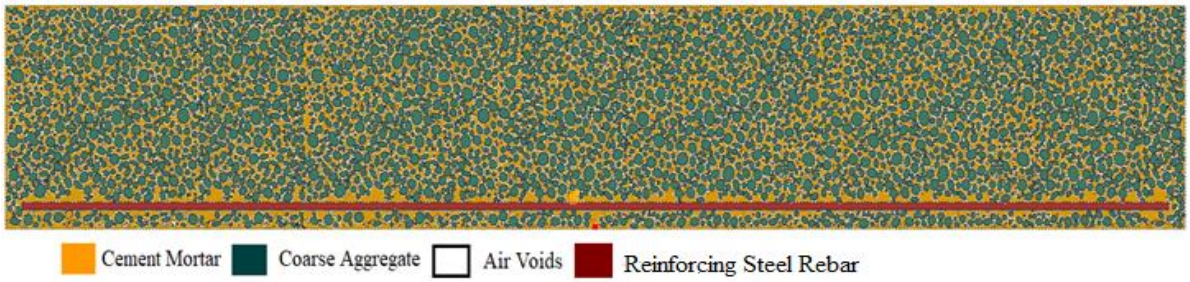

Figure 9. Mesoscale finite element modeling for round coarse aggregate with maximum size 25

Table 3. Materials properties input in ABAQUS program

Material	Modulus of Elasticity, MPa	Poisson's Ratio	Fracture Energy N-mm/mm^2
Aggregate	75000	0.2	-
Mortar	25000	0.2	0.06
Steel	200000	0.3	-

At the beginning, programming in ABAQUS program using PYTHON language was employed for beam modeling. The model is defined as a sketch and takes a name and dimension where this sketch was defined as a rectangular having the same dimension of the beams in 2D to facilitate the process of inserting aggregate in it. In the case of rounded aggregate, it is needed to make excel sheets for each gradient of the aggregate of the same maximum size. For rounded coarse aggregate with maximum size 25 mm it was needed to make 6 excel sheets; one for each gradient and the last one for air voids. The rounded aggregate and air voids will be assumed to be of elliptical shape. This representation has a good accuracy because the rounded aggregate particles are actually not circles.

In the middle span of the RC beams, a notch as high as 4 mm was created. This notch is modeled as a wire part and makes it as the initial crack, and allows for crack growth through the cement mortar. The element type used for the numerical models was a two-dimensional quadrilateral four-noded element of size approximately equal to 1.5 mm side length. In the present study, one should avoid using the triangle element because this element provides results with less accuracy than that of a quadrilateral element as recommended in Huynh et al. (2019) studies [18].

Figures 10 and 11 represent flowcharts to calculate the course aggregate required for each gradient and modeling stage before analyzing it in ABAQUS program, respectively.

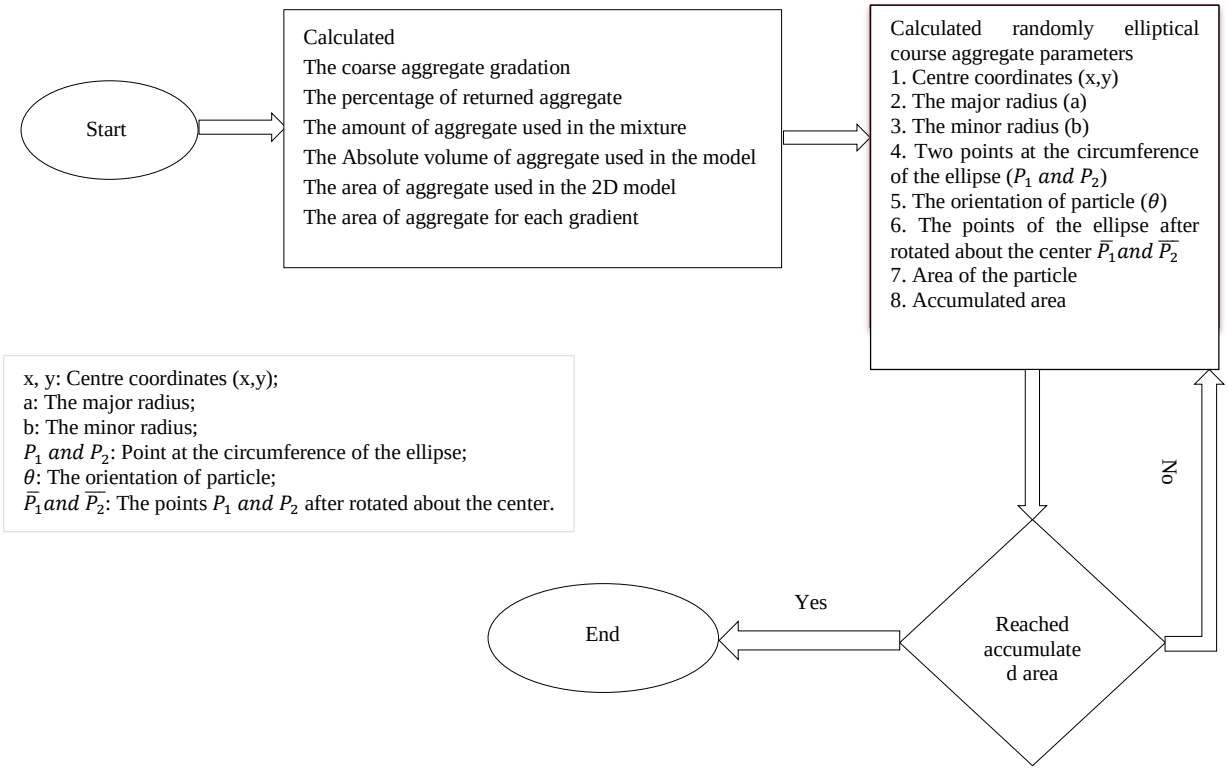

Figure 10. Flowchart to calculate the coarse aggregate required for each gradient

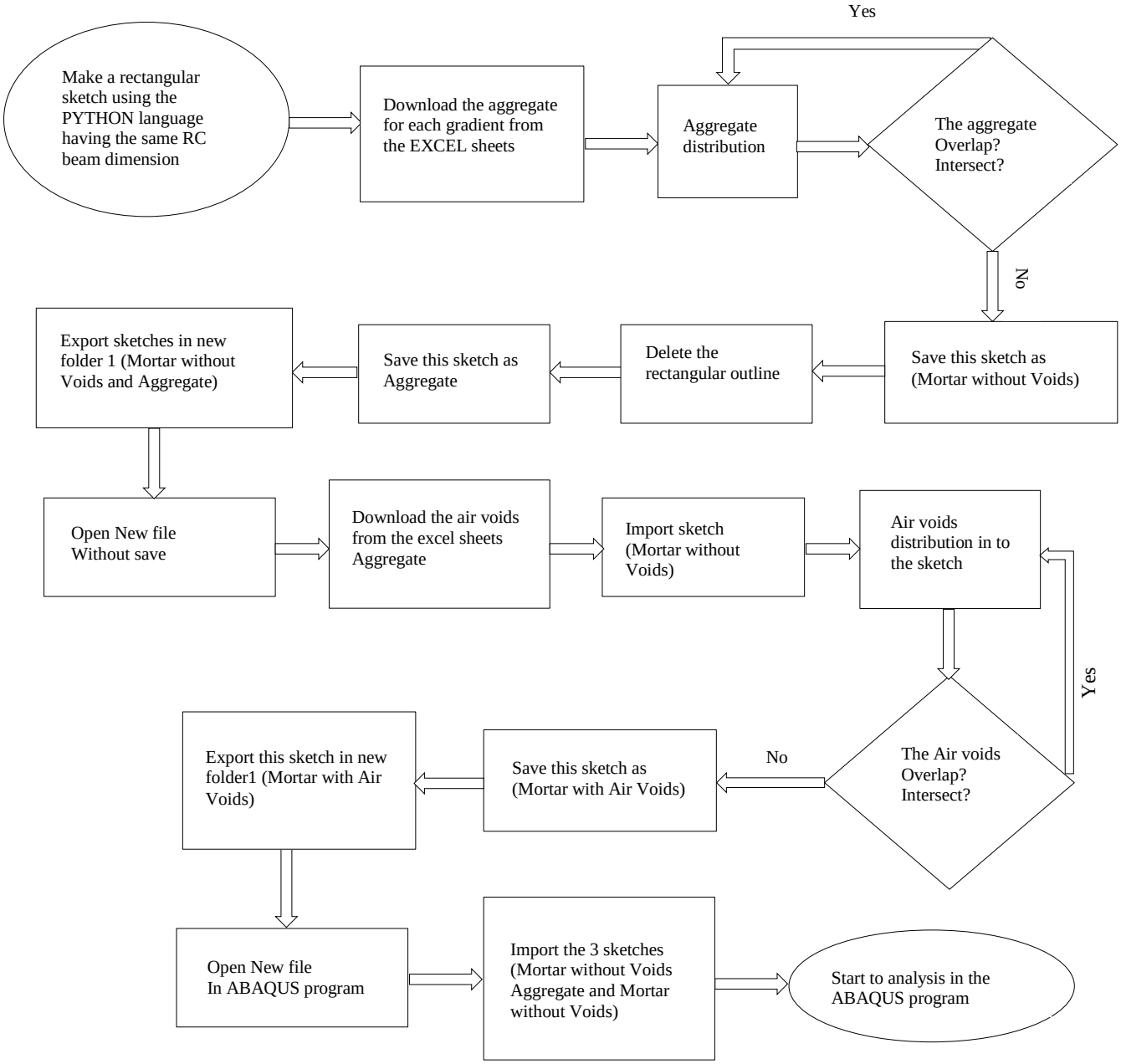

Figure 11. Flowchart of processing modelling at ABAQUS program to start analysis

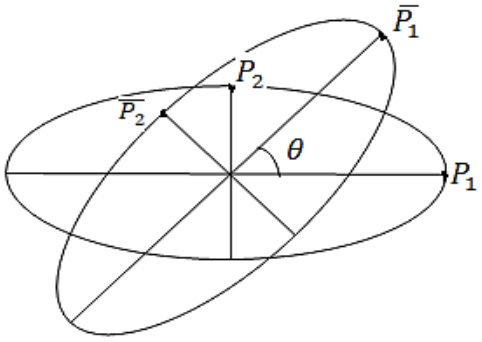

Figure 12. Rotating the ellipse about the centre

6. Results and Discussion

Reinforced concrete beam subjected to a two-point loading was numerically analyzed using a two-dimensional plane stress model to study the non-smooth behavior such as discontinuities and singularities. The effectiveness of the

mesoscale appears in concrete modeling to take its non-homogeneity into account. The numerical analysis was done using the ABAQUS program. In addition, an experimental program was used to detect the reliability of the numerical results of XFEM. Table 4 explains the experimental and numerical maximum applied load for RC beams.

Table 4. The maximum applied load.

Beam Code No.	Experimental work (kN)	Numerical analysis (kN)
17-M 25-R	88.7	100
34-M 25-R	112	130

From Table (4), it can be noted that the beam 34-M 25-R is stronger than the other one. Also, it can be seen that when increasing the concrete compressive strength the maximum applied load (ultimate load) in numerical analysis is approaching from the ultimate experimental applied load.

Note: the percentage of convergence measured at serviceable load (70% for ultimate load).

Performed Figure 13 and Figure 14. The load deflection curve at the mid-span of the beam constructed using aggregate with a maximum size of 25 mm and different compressive strengths 17 MPa and 34 Mpa, respectively, was performed.

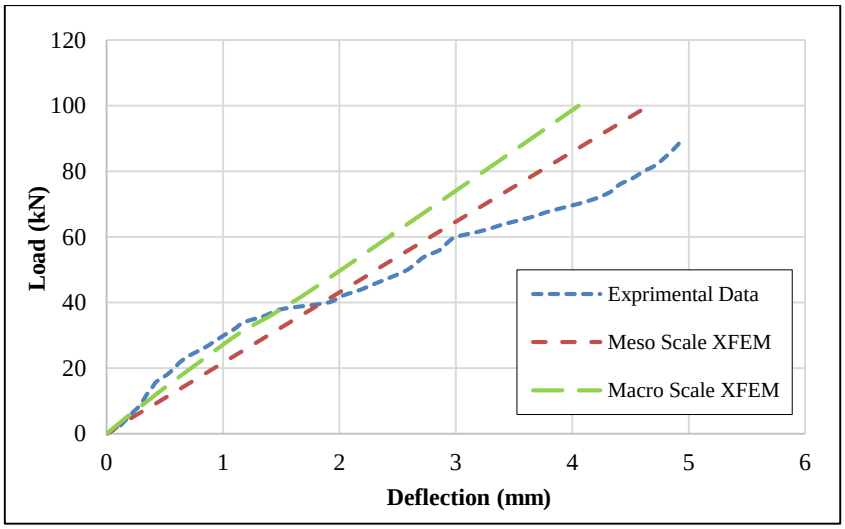

Figure 13. Load – deflection curves for reinforced concrete beam (17-M 25-R)

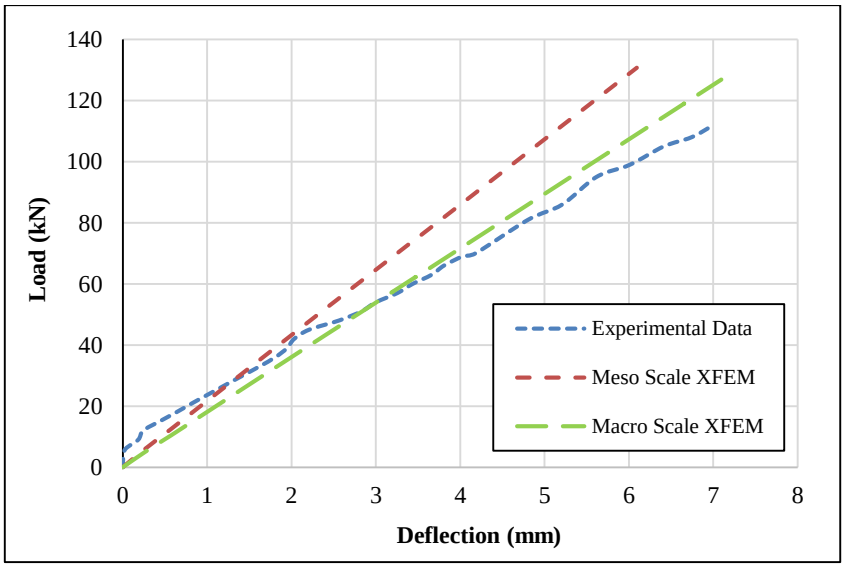

Figure 14. Load – deflection curves for reinforced concrete beam (34-M 25-R)

As can be seen in the above figures, the maximum deflection value obtained for RC beam 34-M 25-R ranged between 6 and 7mm for experimental and numerical results, while the minimum deflection obtained was for RC beam 34-M 25-R which ranged between 4 and 5 mm) in experimental and numerical results.

The fracture energy of the concrete beam can be calculated by computing the area under the curve of applied load and the deflection (area under load-deflection curve) [19]. From the above figures the larger deflection obtained will, gives a larger fracture energy for the RC beam under the applied load. Fractures in material mean, energy required to create a new surface. From the above it is indicated that the fracture energy increased when the compressive strength of the concrete is increased [20]. This is due to the increase in the compressive strength mean increasing in hardness which in turn need a larger fracture energy to create crack and then allow to propagation. In additional to the fracture toughness increases with a decrease in water-to-cement ratio [21)]. From the above the RC beam 34-M 25-R has the largest fracture energy

From Figure 13, when the compressive strength is equal to 17 MPa, the percentage of convergence between the experimental and the numerical mesoscale modeling is equal to 94%, while the percentage decreases to become 81% when the experimental results are compared with the macroscale model result. Furthermore, from Figure 14, when using compressive strength equal to 34 MPa, it will be observed that the percentage of convergence increased between the experimental and the numerical macroscale modeling where it will become equal to 96%, while the percentage of convergence between the experimental and the numerical mesoscale modeling decreases to become 78%.

The relations between the applied load and measured tensile strain at mid-span for beams with compressive strengths of 17 MPa and 34 MPa, are shown in Figures 15 and 16, respectively, while Figure 17 explains the effect of the compressive strength on the increase of the results.

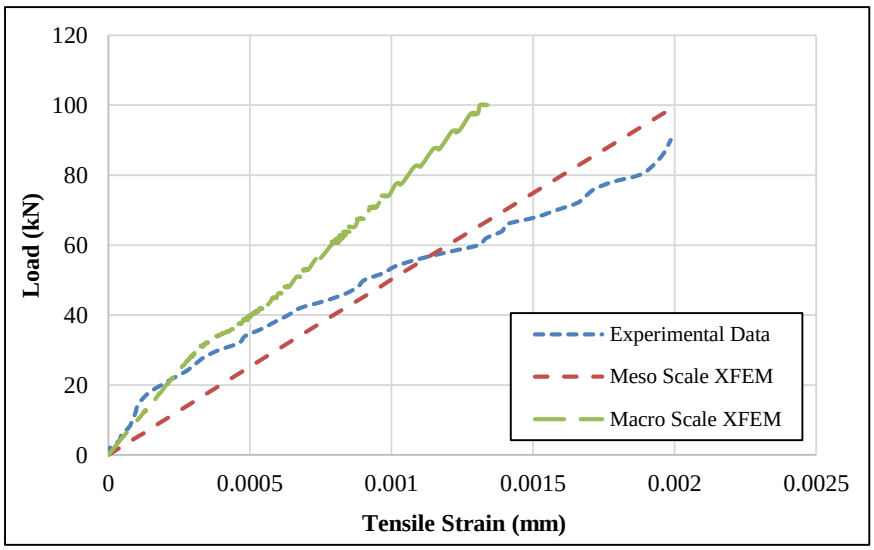

Figure 15. Load –tensile strain curves for reinforced concrete beam (17-M 25-R)

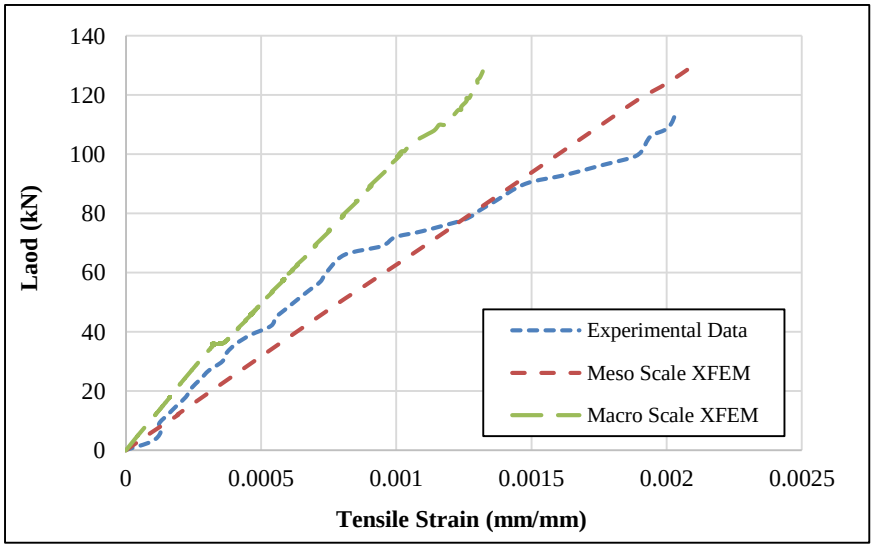

Figure 16. Load–tensile strain curves for reinforced concrete beam (34-M 25-R)

From the curves of the mesoscale figure, it can be seen that the finite element analysis gives more accurate results comparing with the experimental result. Where the percentage of convergence is equal to 93% and 94% for compressive strengths 17 and 34 MPa, respectively, while a divergence in the results of experimental and macroscale can be seen

where the percentage up to 64% for a beam have compressive strength 17 MPa and 41% for the other beam. This indicates that the mesoscale analysis has a convergent behavior to the experiment in the tensile strain measurement. This convergence explains the effectiveness of the mesoscale model for modeling a reinforced concrete beam.

From Figures 15 and 16, tortuous in the curves of the macroscale was seen which may be attributed to the approximation in the concrete modeling when it is assumed as one of the materials that allow propagation of a crack through the concrete with the load increasing.

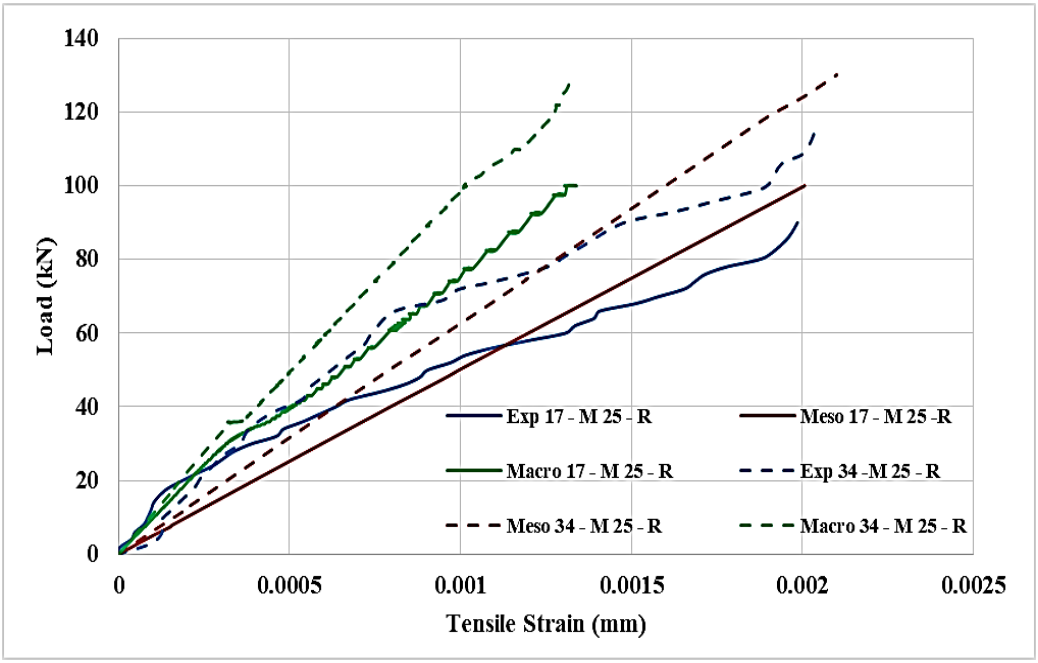

Figure 17. Load – tensile strain curves for RC beams

From the above figure it can be noted that the maximum strain value occurs in the RC beam 34 M 25-R at the ultimate load. When the compressive strength is decreased, the strain value is increased at the same load for experimental and numerical meso and macroscale models. Mesoscale numerical strain result exhibited a good agreement when compared with the same experimental RC beams.

The load-shear strain curves for the numerical (meso and macroscale) and experimental data are shown in Figures 18 and 19.

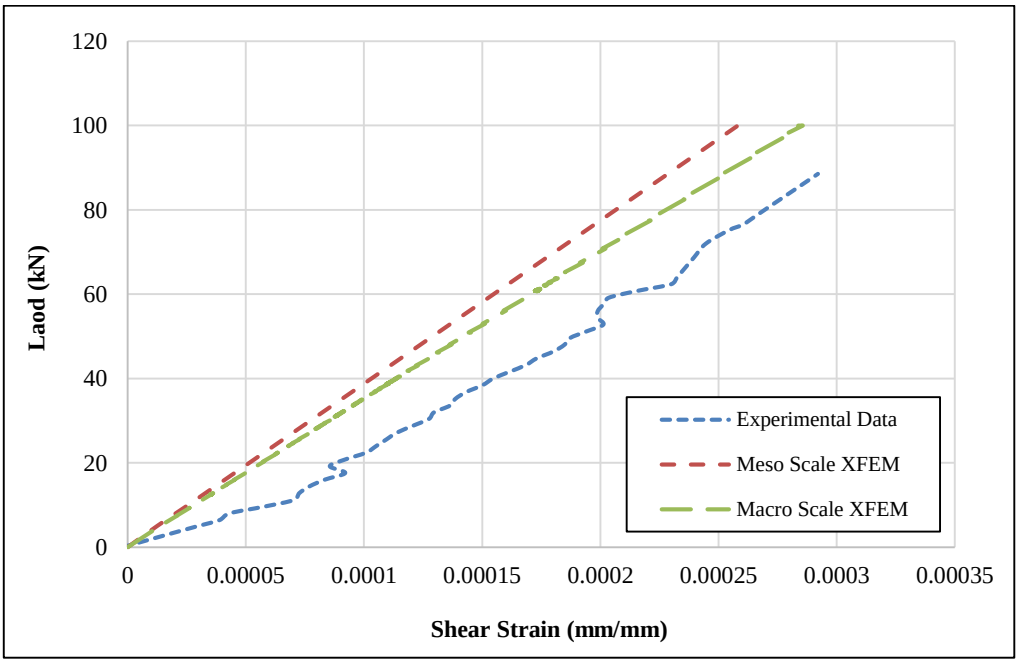

Figure 18. Load – shear strain curves for reinforced concrete beam (17-M 25-R)

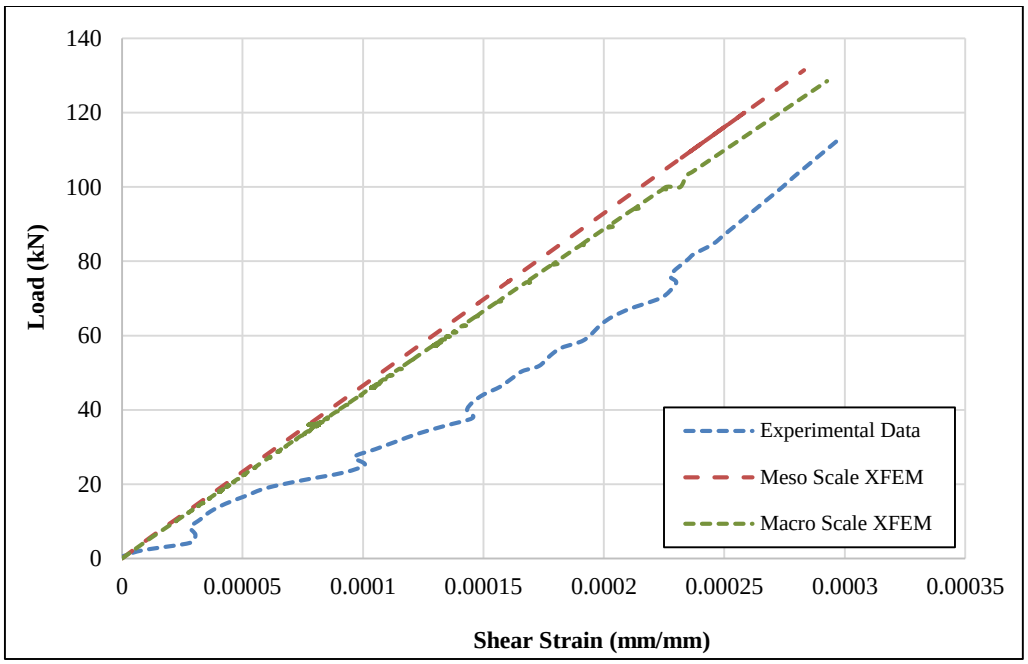

Figure 19. Load – shear strain curves -for reinforced concrete beam (34-M 25-R)

As shown in these figures, all the numerically predicted shear strains change linearly with the increasing of the applied load, while the experimental does not. The maximum values for the shear strain was between 0.0002 mm/mm and 0.00029 mm/mm. Generally, macroscale XFEM modeling gets a percentage of convergence between 91 and 98% if compared with mesoscale at the same load. The percentage of convergence between the experimental and mesoscale numerical analysis reach to 73 and 75% for beams with compressive strength of 17 MPa and 34 MPa, respectively, while this percentage reached up to 78 and 76% if compared with the macroscale numerical analysis. Consequently, the mesoscale numerical modelling was more appropriate to represent the non-homogeneity of the concrete.

7. Conclusions

- The XFEM is a powerful method based on the FE method to treatment discontinuity in the reinforced concrete under flexural result from the cracking phenomenon.
- Mesoscale model was found to be a good process for representing the non-homogeneity of the concrete which it neglected in the macroscale modeling of concrete members. In addition, it shows the importance of the non-homogeneity concrete properties on the behavior of RC beams.
- The crack propagation path of the concrete is affected by the tensile strength of the mortar and location of aggregate particle where the crack passes through the cement mortar only.
- The analysis of the tensile strain behavior in the mesoscale model gave 93 and 96% convergence with the experimental data, while in the macroscale analysis, the tensile strength has a divergent behavior with the experimental data.

8. Conflicts of Interest

The authors declare no conflict of interest.

9. References

[1] Murayama, Yoshimasa. “Mesoscopic Systems” (August 29, 2001). doi:10.1002/9783527618026.

[2] Liao, Kuo-Yu, Ping-Kun Chang, Yaw-Nan Peng, and Chih-Chang Yang. “A Study on Characteristics of Interfacial Transition Zone in Concrete.” Cement and Concrete Research 34, no. 6 (June 2004): 977–989. doi:10.1016/j.cemconres.2003.11.019.

[3] Nitka, M., and J. Tejchman. “Modelling of Concrete Behaviour in Uniaxial Compression and Tension with DEM.” Granular Matter 17, no. 1 (January 28, 2015): 145–164. doi:10.1007/s10035-015-0546-4.

[4] Bentz, D.P., E.J. Garboczi, H.M. Jennings, and D.A. Quenard. “Multi-Scale Digital-Image-Based Modelling of Cement-Based Materials.” MRS Proceedings 370 (January 1994). doi:10.1557/proc-370-33.

[5] Mostafavi, M., N. Baimpas, E. Tarleton, R.C. Atwood, S.A. McDonald, A.M. Korsunsky, and T.J. Marrow. "Three-Dimensional Crack Observation, Quantification and Simulation in a Quasi-Brittle Material." Acta Materialia 61, no. 16 (September 2013): 6276–6289. doi:10.1016/j.actamat.2013.07.011.

[6] Jivkov, Andrey P., Dirk L. Engelberg, Robert Stein, and Mihail Petkovski. "Pore Space and Brittle Damage Evolution in Concrete." Engineering Fracture Mechanics 110 (September 2013): 378–395. doi:10.1016/j.engfracmech.2013.05.007.

[7] Schlangen, E., and E.J. Garboczi. "Fracture Simulations of Concrete Using Lattice Models: Computational Aspects." Engineering Fracture Mechanics 57, no. 2–3 (May 1997): 319–332. doi:10.1016/s0013-7944(97)00010-6.

[8] Wang, Xiaofeng, Mingzhong Zhang, and Andrey P. Jivkov. "Computational Technology for Analysis of 3D Meso-Structure Effects on Damage and Failure of Concrete." International Journal of Solids and Structures 80 (February 2016): 310–333. doi:10.1016/j.ijsolstr.2015.11.018.

[9] Al-Zuhairi, Alaa H., and Ali Ihsan Taj. "Finite Element Analysis of Concrete Beam under Flexural Stresses Using Meso-Scale Model." Civil Engineering Journal 4, no. 6 (July 4, 2018): 1288. doi:10.28991/cej-0309173.

[10] Mohammadi, Soheil, ed. "Extended Finite Element Method" (January 1, 2008). doi:10.1002/9780470697795.

[11] Pommier, Sylvie, Anthony Gravouil, Alain Combescure, and Nicolas Moës. "Extended Finite Element Method X-FEM." Extended Finite Element Method for Crack Propagation (March 7, 2013): 69–108. doi:10.1002/9781118622650.ch3.

[12] Mohammadi, Soheil, ed. "Extended Finite Element Method" (January 1, 2008). doi:10.1002/9780470697795.

[13] Belytschko, Ted, and Tom Black. "Elastic crack growth in finite elements with minimal remeshing." International journal for numerical methods in engineering 45, no. 5 (April 21, 1999): 601-620. doi:10.1002/(sici)1097-0207(19990620)45:5%3C601::aid-nme598%3E3.0.co;2-s.

[14] Liu, Tiejun, Shanshan Qin, Dujian Zou, Wen Song, and Jun Teng. "Mesoscopic Modeling Method of Concrete Based on Statistical Analysis of CT Images." Construction and Building Materials 192 (December 2018): 429–441. doi:10.1016/j.conbuildmat.2018.10.136.

[15] Yang, Xu, and Fenglai Wang. "Random-Fractal-Method-Based Generation of Meso-Model for Concrete Aggregates." Powder Technology 284 (November 2015): 63–77. doi:10.1016/j.powtec.2015.06.045.

[16] Kim, Han-Soo, and Geon-Hyeong Kim. "Enriched Degree of Freedom Locking in Crack Analysis Using the Extended Finite Element Method." Advances in Mechanical Engineering 11, no. 6 (June 2019): 168781401985979. doi:10.1177/1687814019859793.

[17] Wang, X.F., Z.J. Yang, J.R. Yates, A.P. Jivkov, and Ch Zhang. "Monte Carlo Simulations of Mesoscale Fracture Modeling of Concrete with Random Aggregates and Pores." Construction and Building Materials 75 (January 2015): 35–45. doi:10.1016/j.conbuildmat.2014.09.069.

[18] Huynh, Hai D., Phuong Tran, Xiaoying Zhuang, and H. Nguyen-Xuan. "An Extended Polygonal Finite Element Method for Large Deformation Fracture Analysis." Engineering Fracture Mechanics 209 (March 2019): 344–368. doi:10.1016/j.engfracmech.2019.01.024.

[19] Bazant, Z.P. "Fracture Mechanics of Concrete Structures" (April 21, 2014). doi:10.1201/9781482286847.

[20] Rozalija Kozul and David Darwin "Effects of aggregate type, size, and content on concrete strength and fracture energy" (June 1997) The National Science Foundation Research Grants No. MSS-9021066 and CMS-9402563.

[21] Nallathambi, P., B. L. Karihaloo, and B. S. Heaton. "Effect of Specimen and Crack Sizes, Water/cement Ratio and Coarse Aggregate Texture upon Fracture Toughness of Concrete." Magazine of Concrete Research 36, no. 129 (December 1984): 227–236. doi:10.1680/macr.1984.36.129.227.